Dynamic Behavior of Local Solids Concentration in Fluidized Beds: Experimental Validation of an Eulerian-Eulerian Model

Clay R. Sutton and John C. Chen
Department of Chemical Engineering
Lehigh University
Bethlehem, PA 18015

ABSTRACT

Recent years have witnessed significant improvements in the computer modeling of fluidized particle systems. Such models hold the potential to simulate complex systems and thus greatly reduce design efforts. As we approach the goal of simulating arbitrary systems, there exists a greater need to challenge the ability of the models to predict key features of operating beds. The simplest challenge is to predict global time average properties such as the pressure gradient and bed expansion. The next level of detail is prediction of local time average characteristics such as the solids fraction at a specified location. A third level is the prediction of dynamic characteristics of *local* behavior, which has important implications for heat and mass transfer processes, reaction kinetics, and mixing. Our aim is to investigate the ability of an Eulerian-Eulerian (two-fluid) model to predict local fluctuations in the solids phase concentration.

Experimentally we utilize needle-capacitance probes to measure time series transients of local solids fraction. The Eulerian-Eulerian model selected for this validation test is the MFIX CFD package (www.mfix.org). Two closures for the interphase momentum transfer coefficient are adopted, the first empirical (a combination of Ergun (1), and Wen and Yu (2)) and the second due to Koch and Hill (3) estimated from lattice-Boltzmann simulations. For validation purposes we look at the dynamic behavior of the experimental and model solids fraction transients. While statistical and spectral features of the artificial signals compare favorably with experiment, local dynamic features are not captured very well. Three reasons account for this: 1) the model does not predict expansion in the emulsion, 2) the model does not capture small-scale density fluctuations in the emulsion, and 3) the model does not correctly predict the bubble to wake transition.

INTRODUCTION

Many of the phenomena observed in fluidized beds depend strongly on the local dynamic behavior. Time averaged behavior alone is not sufficient to explain many experimental observations. The presence of heterogeneous structure such as bubbles or clusters can significantly affect microscopic processes such as transport, reaction kinetics and mixing, while at the same time having a relatively small impact on local time averaged properties such as solids holdup. The bubbling bed model of Kunii and Levenspiel (4) takes into account local heterogeneous structure, and was the first model to successfully capture heat and mass transfer between phases. Numerous experimental studies in various types of fluidized beds demonstrate that local Nusselt and Sherwood numbers have a dependence on heterogeneous structure (e.g., 5, 6). Reaction kinetics is also strongly related to the presence of heterogeneous structure. For example the presence of particles in the dilute phase can account for a significant portion of the conversion (7). Solids mixing can also affect transport

and kinetic processes as well as phenomena such as segregation (4), but it too depends on the presence of heterogeneous structures; in bubbling beds most solids mixing is due to circulation in the bubble wake region (4). The only way to fully understand these phenomena, therefore, is to understand the local transient behavior.

Likewise, successful determination of design parameters such as heat exchanger requirements and reactant conversions requires that fluidization models accurately predict local transient behaviors. As such it is crucial to validate fluidization models at the local scale (one to two orders of magnitude less than the vessel scale). This work is aimed at assessing the ability of an Eulerian-Eulerian (Two-Fluid Model, TFM) type fluidization model (e.g., 8) to predict local bed behavior by comparing experimentally measured local solids fraction time series with those generated from a typical TFM CFD code.

The future of modeling fluidized particle systems no doubt lies in Lagrangian-Eulerian type models such as molecular dynamics (MD) (e.g., 9), discrete particle models (DPM) (e.g., 10) and discrete element methods (DEM) (e.g., 11), but these models are still limited to small-scale studies ($<10^6$ particles). Despite the great strides made in development of faster microprocessors, the Eulerian-Eulerian Two-Fluid Model still represents our best hope for simulating large-scale gas-solid systems with present day computational resources. Qualitatively the TFM has captured phenomena such as bubble shape, segregation and bed inversion (12). Global quantitative behavior such as bed expansion (e.g., 13), bubble size and rise velocity (14), pressure fluctuations, and global dynamic characteristics (15) have also been predicted by the Eulerian-Euerian model. However, comprehensive validation of the transient behavior on a local level is still lacking in the literature. Quoting Grace and Taghipour (16), "great care is required to verify computational aspects of the model and to plan and execute proper experimental validation tests." This work is believed to be the first to attempt quantitative validation of the TFM in terms of local dynamics.

SIMULATION

The Two-Fluid Model is implemented using the MFIX code developed at the Morgantown Energy Technology Center (www.mfix.org). Full details of the model are well described in the MFIX Theory Guide (8) and will not be elaborated on here. Simulations were carried out in 2-D Cartesian space and the geometry was chosen to represent the experimental system described in the following section. Grid refinement was studied by examining the time average axial solids fraction profiles. The Superbee second order method was applied for discretization. The initial and boundary conditions applied were similar to those used by Van Wachem et al. (13). An algebraic version of the granular energy equation was used due to Syamlal (17) who argued

Table 1 – Model Parameters

Symbol	Description	Value
ρ_s	Solids density	2450 kg/m^3
d_p	Particle diameter	522 μm
e_p	Particle restitution	0.80
ε_p	Voidage at max. packing	0.38
ϕ	Angle of internal friction	25º
M_g	Molecular weight of gas (air)	29.0 kg/kmol
μ_g	Viscosity of gas	1.79x10^{-5} Pa·s
U_0	Superficial gas velocity	0.295 m/s
H_c	Column height	0.5 m
H_s	Settled bed height	0.3 m
W_c	Column width	0.23 m
Δt	Time step	1x10^{-4} s
Δt_{min}	Min. time step	1x10^{-7} s
$\Delta x = \Delta y$	Mesh spacing	0.333 cm
T	Temperature	300 K

that in dense-phase fluidization, granular energy is dissipated locally, and hence the convective and diffusive terms may be neglected in the full energy balance. This results in great computational savings. Table 1 summarizes simulation parameters.

For comparison purposes with experiment, the simulations were run until the bed reached fully expanded height, and the initial numerical symmetry was broken. Next, solids fraction data were logged at a frequency of 300Hz for a period of 60sec (18,000 data points). Computational cells corresponding to measurement locations in the experimental system were averaged with all eight adjacent cells in order to approximate the actual probe measurement volume.

Gas-Solid Drag Force

Closure of the interphase momentum transport term remains a major challenge to the modeling community. The nature of heterogeneous structures predicted by simulation is extremely sensitive to the choice of drag law (9). In light of this we employ two different types of drag relations in this work, the first of an empirical nature, and the second an explicit closure determined by direct numerical simulation. The transfer of momentum between phases is typically modeled using empirical relations of an Ergun type (1) obtained from pressure drop data in fixed beds, or a Richardson-Zaki type (18) determined from bed expansion data. While Ergun's equation is adequate for describing relatively dense suspensions, it fails at higher void fractions and an empirical relation of the Richardson-Zaki type is more appropriate such as that due to Wen and Yu (2). Despite the highly empirical nature of these relations, they have proven very successful at predicting many important features of fluidized beds including minimum fluidization velocities and solids entrainment. The drag function (β) in this case is defined as:

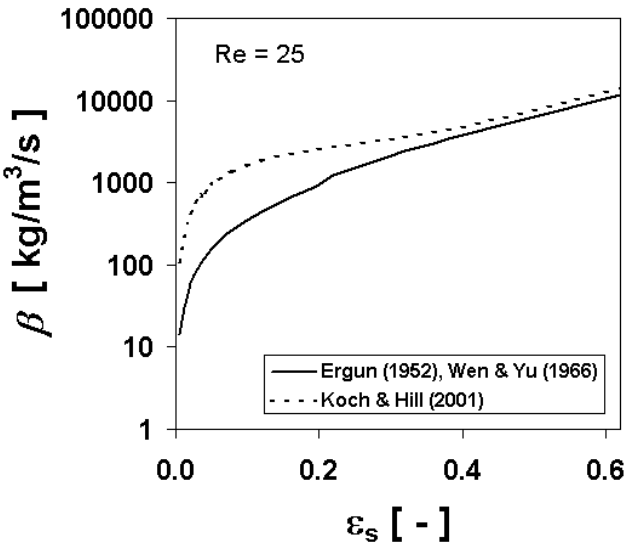

Figure 1 – Variation of drag function (β) with solids concentration at constant Reynolds Number

$$\beta = \begin{cases} 150\dfrac{\varepsilon_s^2 \mu_g}{\varepsilon d_p^2} + 1.75\dfrac{\varepsilon_s \rho_g \left| v_g - v_s \right|}{d_p}, & \text{for } \varepsilon < 0.8 \\ \dfrac{3}{4} C_D \dfrac{\varepsilon \varepsilon_s \rho_g \left| v_g - v_s \right|}{d_p} \varepsilon^{-2.65}, & \text{for } \varepsilon \geq 0.8 \end{cases} \quad (1)$$

$$C_D = \begin{cases} \dfrac{24}{\mathrm{Re}_p}\left(1 + 0.15\,\mathrm{Re}_p^{0.687}\right), & \text{for } \mathrm{Re}_p < 1000 \\ 0.44, & \text{for } \mathrm{Re}_p \geq 1000 \end{cases} \quad (2)$$

$$\mathrm{Re}_p = \frac{\varepsilon \rho_g |v_g - v_s| d_p}{\mu_g} \tag{3}$$

A relatively new approach towards developing closure relations is to use direct numerical techniques employing only first principles. These types of drag formulations have an advantage in that they require no empirical fitting parameters. Koch and Hill (3) recently reported an explicit closure for the interphase momentum transfer. They estimated drag force on particle assemblies from lattice-Boltzmann simulations. This closure has been applied to MD (9), TFM and DPM (19) type simulations.

$$\beta = \begin{cases} \dfrac{18\mu\varepsilon^2\varepsilon_s}{d_p^2}\left[F_0(\varepsilon_s) + F_1(\varepsilon_s)\mathrm{Re}_{kh}^2\right], & \text{for } \mathrm{Re}_{\mathrm{kh}} < 20 \\ \dfrac{18\mu\varepsilon^2\varepsilon_s}{d_p^2}\left[F_0(\varepsilon_s) + F_3(\varepsilon_s)\mathrm{Re}_{kh}\right], & \text{for } \mathrm{Re}_{\mathrm{kh}} \geq 20 \end{cases} \tag{4}$$

$$F_0 = \begin{cases} \dfrac{1 + 3(\varepsilon_s/2)^{1/2} + (135/64)\varepsilon_s \ln\varepsilon_s + 16.14\varepsilon_s}{1 + 0.681\varepsilon_s - 8.48\varepsilon_s^2 + 8.16\varepsilon_s^3}, & \text{for } \varepsilon_s < 0.4 \\ \dfrac{10\varepsilon_s}{(1-\varepsilon_s)^3}, & \text{for } \varepsilon_s \geq 0.4 \end{cases} \tag{5}$$

$$F_1 = 0.110 + 5.10\times10^{-4}\exp[11.6\varepsilon_s] \tag{6}$$

$$F_3 = 0.0673 + 0.212\varepsilon_s + \frac{0.0282}{(1+\varepsilon_s)^5} \tag{7}$$

$$\mathrm{Re}_{kh} = \frac{\varepsilon\rho_g|v_g - v_s|d_p}{2\mu_g} \tag{8}$$

The variation of the drag functions (β) with solids density is shown in Fig 1. For both approaches it is seen that at this particle Reynolds number, the two drag functions are in agreement at high solids concentrations, but differ significantly for ε_s less than 0.4.

EXPERIMENT

The experimental apparatus is shown in Fig 2 and described in detail elsewhere (20). The system is summarized in Table 2. 522μm mean diameter glass beads were chosen as the fluidization media. These particles are defined unambiguously as Geldart-B, yielding good bubbling behavior. Furthermore the effect of

Table 2 – Experimental Parameters

Symbol	Description	Value
ρ_s	Solids density	2450 kg/m^3
d_p	Particle diameter	522 μm
U_0	Superficial gas velocity	0.295 m/s
H_c	Column height	0.5 m
H_s	Settled bed height	0.3 m
W_c	Column width	0.23 m
D_c	Column depth	0.14 m
$Z_{1,2,3}$	Probe locations (above grid)	2.54, 10.16, 17.15 cm

interparticle cohesiveness is minimal. The test case experiment was performed at a settled bed height H_s = 30cm and a superficial gas velocity U_0 = 29.5cm/s. Needle-capacitance probes (e.g., 20) were utilized to measure local instantaneous solids fraction transients. The measurement volume for each probe is approximately equal to a conical region with base diameter 6.4mm and height 12.7mm. Solids density transients at three axial heights (z = 2.54, 10.16, 17.15cm above the distributor plate) were logged simultaneously at a frequency of 300Hz for 60sec. The probes were inserted to the center of the bed widthwise in order to minimize wall effects.

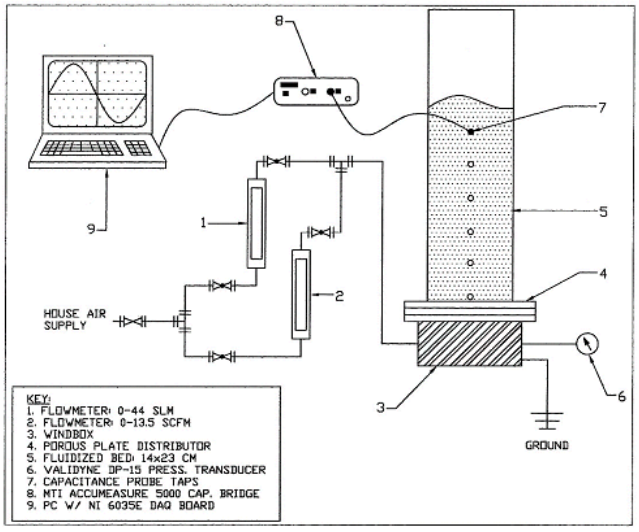

Figure 2 – Experimental apparatus

RESULTS AND DISCUSSION

Simulations employing both the empirical (Ergun combined with Wen and Yu) and explicit (Koch and Hill) drag closures predict comparable bed expansion (the explicit model predicts slightly higher expansion). Visually the simulations are very encouraging (Fig 3). The simulations capture the classic kidney shaped bubbles. The explicit drag model predicts a greater presence of solids within the bubble phase than does the empirical model, indicating that the two models would predict significantly different conversions for catalytic processes (7). Typical time series of local instantaneous solids density (Fig 4) exhibit a glaring difference the between experiment and models; the models do not capture expansion and small-scale fluctuations in the dense emulsion.

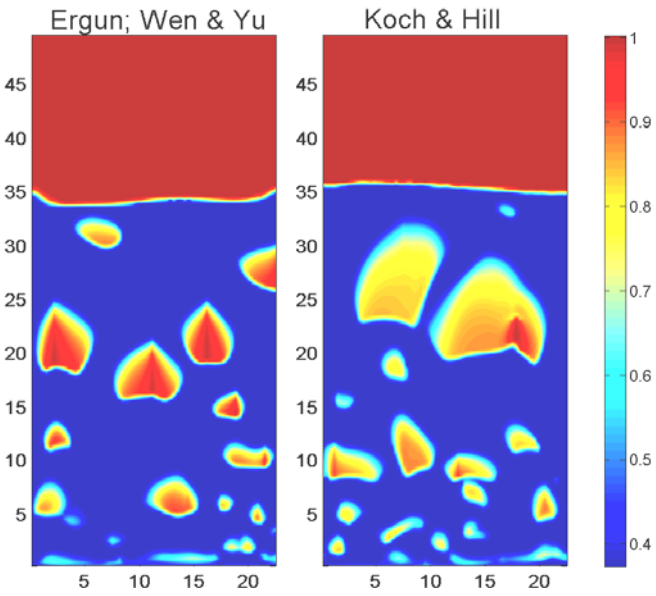

Figure 3 – Snapshots of voidage for two different drag closures.

Time Domain

The experimentally measured time averaged local solids density is compared with simulation results for both drag models in Fig 5. While the Koch and Hill closure is superior, the simulation overpredicts local solids holdup for both drag laws. In a real fluidized system, the dense emulsion phase expands slightly above the loose packed condition, while in the models, the emulsion does not exhibit this characteristic expansion. This is also borne out in the probability distributions (pdf) for the solids fraction transients (Fig 6). The most significant

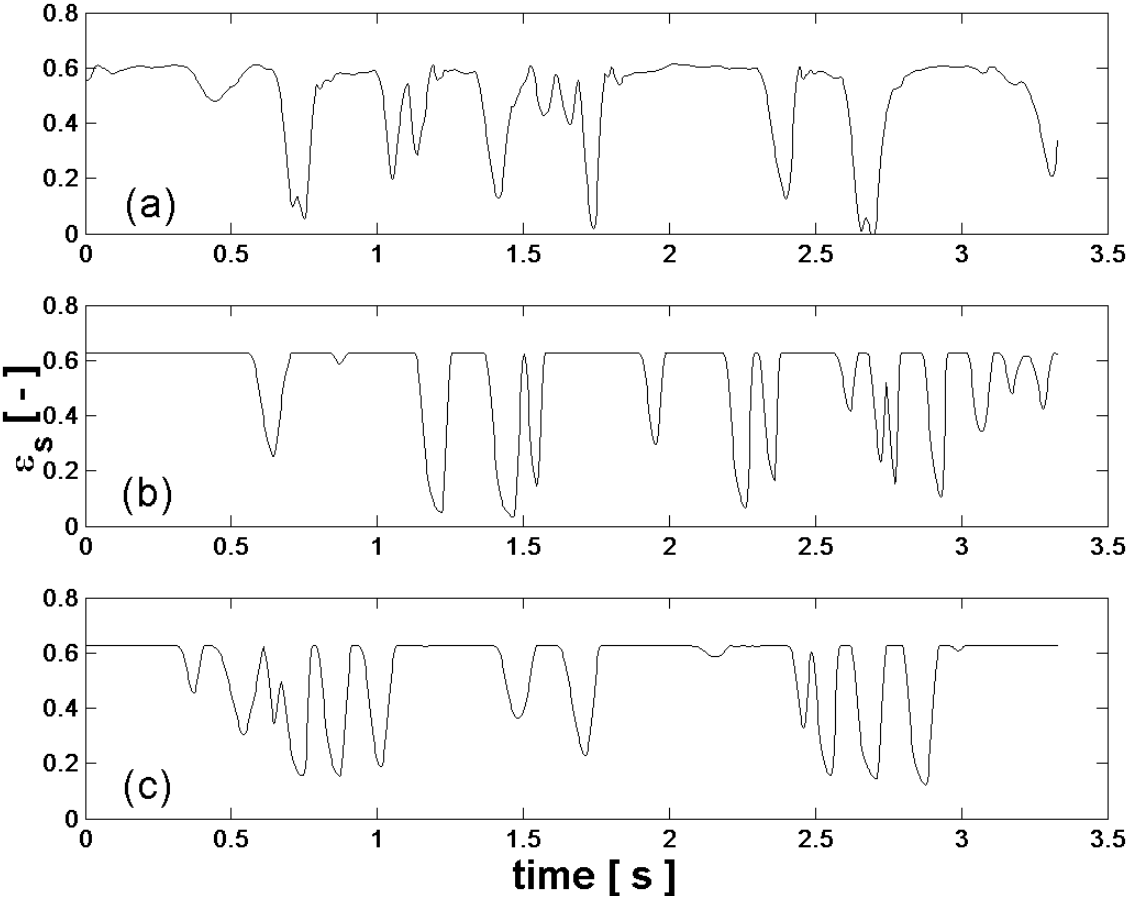

Figure 4 – Typical time traces of solids fraction for (a) experiment, (b) Ergun with Wen and Yu, and (c) Koch and Hill.

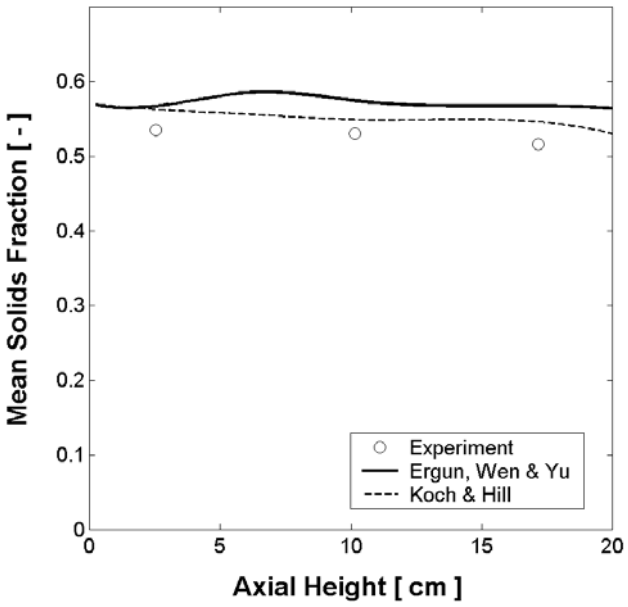

Figure 5 – Axial profiles of time averaged solids concentration.

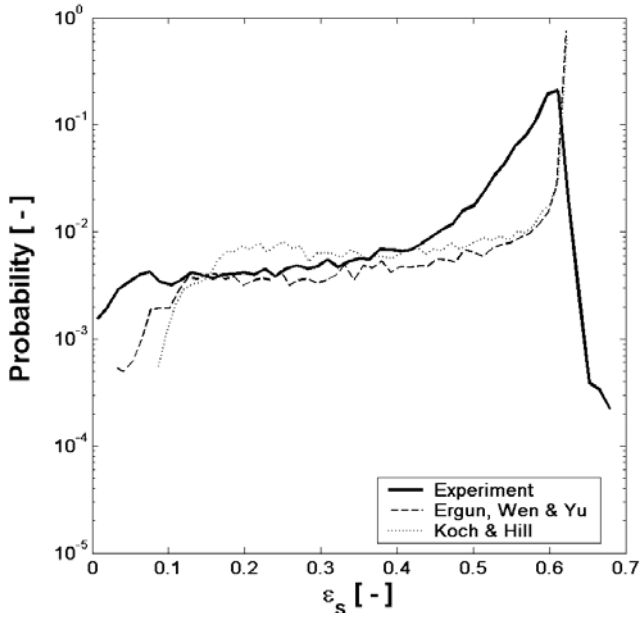

Figure 6 – Probability distributions of solids fraction signals at 10.16cm above the distributor

deviation from the measured and simulated pdf's is in the emulsion region. Note that the peak in the experimental distribution lays below the simulated peaks by about the same difference

the experimental time average solids fraction lies under the simulated time average. Fig 7 displays the standard deviation of the local instantaneous solids fraction. Predicted standard deviations compare quite closely to experiment, which gives us the first indication the model is predicting the macro-scale behavior quantitatively.

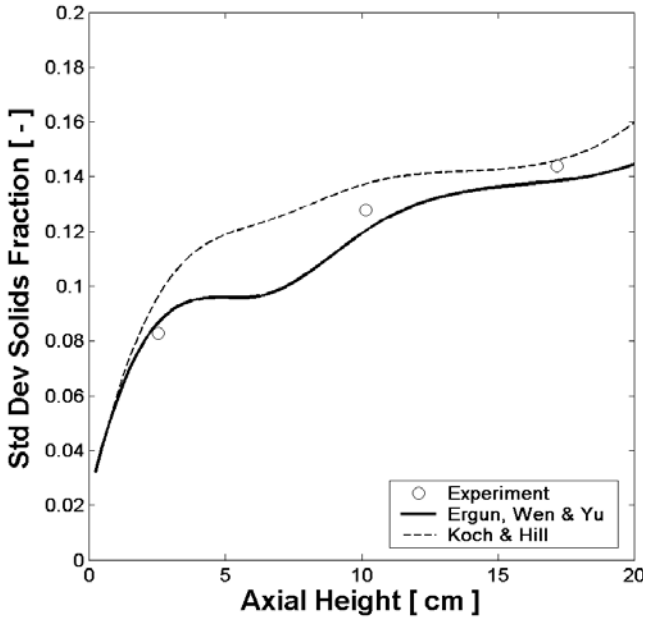

Figure 7 – Axial profile of the solids fraction signal standard devation.

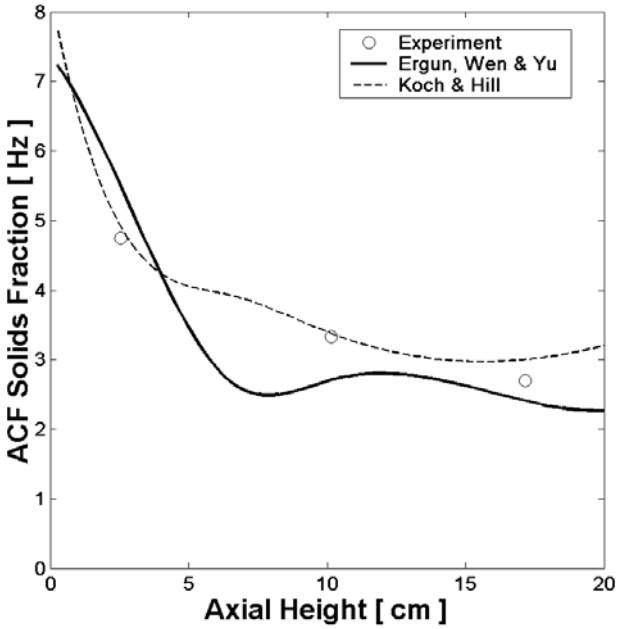

Figure 8 – Axial profiles of the average cycle frequencies for the solids concentration signals.

Frequency Domain

Prediction of average cycle frequency is illustrated in Fig 8. Average cycle frequency is defined as:

$$\mathrm{ACF} = \frac{\#\ \text{of mean crossings}}{2 \times \text{time of observation}} \qquad (12)$$

This is easier to estimate than bubble frequency, and is less subjective because there is no arbitrary decision to make as to what constitutes the existence of a bubble. While simulations performed using both drag closures do quite well, clearly the explicit model of Koch and Hill performs the best at all three axial heights.

Fig 9 displays typical power spectra for experiment and simulation. The experimental spectra contains noise in the higher frequencies probably associated with instrument noise. In the low frequency range below 10Hz there is very good agreement in the frequency domain. Qualitatively the model captures the falloff at higher frequencies. The Koch and Hill drag closure predicts the falloff remarkably well at all axial heights, while the combined Ergun with Wen and Yu model only does well quantitatively at the lowest measurement location.

State-Space Domain

Typical attractors are displayed in Fig 10. Two aspects are missed by the simulation models. First, as noted previously, orbitals corresponding to fluctuations in the dense emulsion are not simulated. Second, there is poor agreement in the second principle component. The second principle component is by definition proportional to the first derivative in time of $\varepsilon_s(x,y,z,t)$, and therefore it is an indicator of how distinct the transition between the

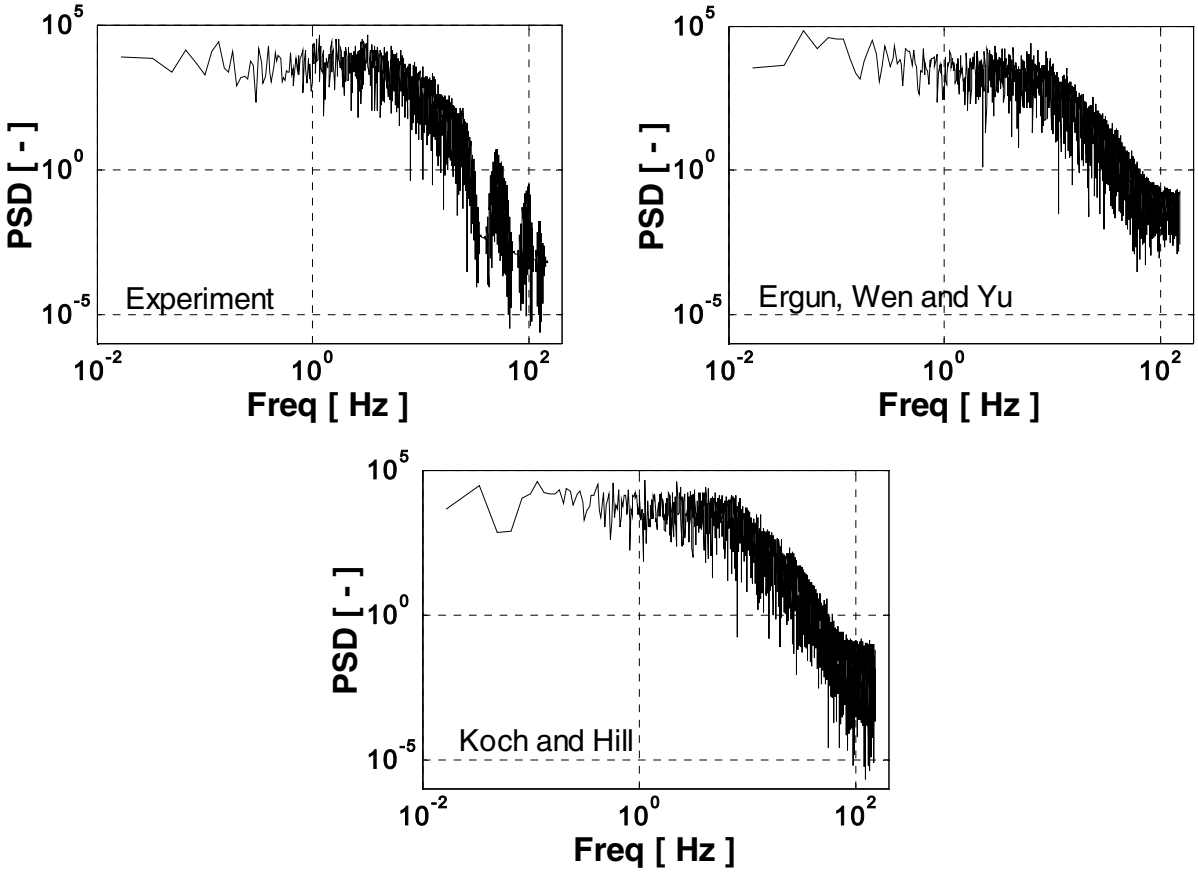

Figure 9 – Power spectra measured 10.16cm above the distributor from experimental and model solids concentration signals.

dense (emulsion) and lean (bubble) phase is. The attractor for solids fraction transients rotates clockwise and thus the lower portion corresponds to the bubble nose, and the upper portion to the bubble wake. The bubble nose transition is predicted well as indicated by the magnitude of the second principle component below the *x*-axis. The model predicts however a much more distinct transition into the wake than is observed experimentally, indicated by high positive values of principle component two. There is better agreement at the lowest axial position where voids are small enough that the probe measurement volume averages out discrepancies in the measured transitions.

Kolmogorov entropies as reported in bits/cycle are severely underpredicted by both models (Fig 11). This is perhaps due to the failure to predict small-scale fluctuations in the emulsion phase. Because there is weak scale separation in the frequency domain between the fluctuations in the emulsion phase and the frequency of macrostructure, it is difficult to estimate the contribution of emulsion phase density fluctuations to the entropy. The high frequency contribution does not appear to contribute significantly to the entropy as evidenced by the power spectra.

SUMMARY

The Eulerian-Eulerian (TFM) model for fluidized beds currently represents our best hope for simulating large-scale systems with present day computational resources. Most existing validation studies in the literature are concerned with the ability of models to predict global time average properties such as bed expansion and bubble shape. However, the local dynamic behavior strongly influences transport processes, reaction kinetics, and mixing in fluidized beds. As such it is crucial to validate the ability of these models to capture local transient behaviors. This study attempts validation of an Eulerian-Eulerian fluidization model by comparison with experimentally measured local solids density transient signals obtained from needle-capacitance probes at several axial heights. Because selection of the drag closure has major implications for the nature of the predicted heterogeneous structure, an empirical closure (combined Ergun with Wen and Yu) and an explicit closure (Koch and Hill) are both adopted.

Statistical, spectral, and dynamic features of the experimental and simulated signals are compared. Statistical time series analysis reveals that the TFM model does not correctly predict expansion in the emulsion phase, as well as characteristic small density fluctuations in the emulsion. Spectral features compare well at low frequencies for both drag closures, but the explicit Koch and Hill closure predicts quantitatively the falloff behavior in the power spectra. The model, with either drag laws, severely underpredicts dynamic behavior as quantified by the Kolmogorov entropy. Examination of attractors reveals that the model predicts a much more distinct transition from bubble to wake than is observed experimentally.

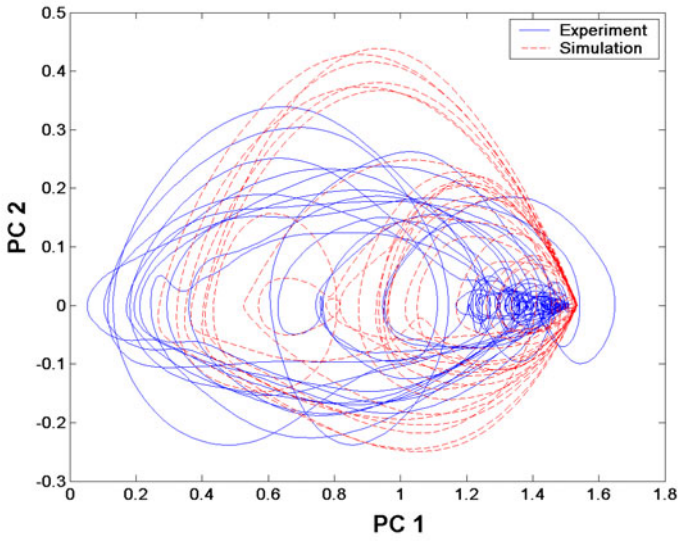

Figure 10 – Typical chaotic attractors reconstructed from solids fraction signals measured 10.16cm above the distributor

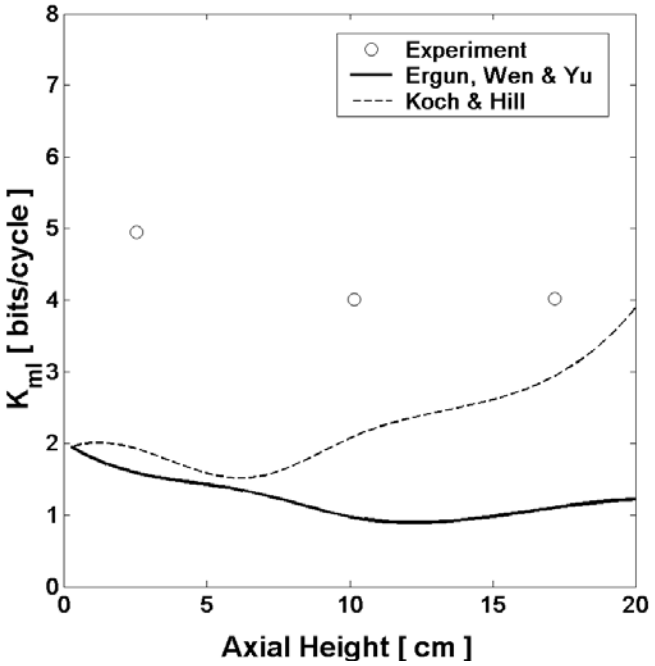

Figure 11 – Axial profiles of the cycle-basis Kolmogorov entropy for the solids concentration signals.

REFERENCES

1. Ergun, S. *Chem. Eng. Progr.*, **48**, 89 (1952).
2. Wen, C.Y. and Y.H. Yu. *AIChE Sym. Series.*, **62**, 100 (1966).
3. Koch, D.L. and R.J. Hill. *Annual Rev. Fluid Mech.*, **33**, 619 (2001).
4. Kunii, D. and O. Levenspiel. *Fluidization Engineering*. (Krieger, Huntington, NY, 1977).
5. Briens, C.L, M. Del Pozo, C. Trudell, and G. Wild. *Chem. Eng. Sci.*, **54**(6), 731 (1999).
6. Li, J., X. Zhang, J. Zhu, and J. Li. *Fluidization IX*. 405 (1998).
7. Sun, G. and J.R. Grace. *Chem. Eng. Sci.* **45**(8), 2187 (1990).
8. Syamlal M., W. Rodgers and T.J. O'Brien. DOE/METC-94/1004, NTIS/DE94000087 (1993).
9. Li, J. and J.A.M. Kuipers. *Chem. Eng. Sci.* **58**(3-6), 711 (2003).
10. Xu, B.H. and A.B. Yu. *Chem. Eng. Sci.* **52**(16), 2785 (1997).
11. Tsuji, Y., T. Kawaguchi and T. Tanaka. *Powder Tech.* **77**, 79 (1993).
12. Van Wachem, B.G.M., J.C. Schouten, C.M. van den Bleek, R. Krishna, and J.L. Sinclair. *AIChE Journal* **47**, 1292 (2001).
13. McKeen, T. and T. Pugsley. *Powder Tech.*, **129**(1-3), 139 (2003).
14. Van Wachem, B.G.M., J.C. Schouten, R. Krishna, and C.M van den Bleek. *Comp. Chem. Eng.* **22**, S299 (1998).
15. Van Wachem, B.G.M., J.C. Schouten, R. Krishna, and C.M van den Bleek. *Chem. Eng. Sci.* **54**(13), 2141 (1999).
16. Grace, J.R. and F. Taghipour. *Powder Tech.* **139**(2), 99 (2004).
17. Syamlal, M. DOE/MC/21353-2373, NTIS/DE87006500 (1987).
18. Richardson, J.F. and W.N. Zaki. *Trans. Inst. Chem. Eng.* **32**, 35 (1954).
19. Bokkers, G.A., M. van sint Annaland, and J.A.M. Kuipers. *Fluidization XI*. 187 (2004).
20. Sutton, C.R. and J.C. Chen. *Ind. Eng. Chem. Res.* **43**(18), 5776 (2004).